

Novel anti-hepatitis B virus-active catechin and epicatechin from *Rhus tripartita*

MOHAMMAD K. PARVEZ¹, MOHAMMED S. AL-DOSARI¹, MAZIN A. S. ABDELWAHID²,
ALI S. ALQAHTANI¹ and ABDULLAH R. ALANZI¹

¹Department of Pharmacognosy, College of Pharmacy, King Saud University, Riyadh 11451, Saudi Arabia; ²Department of Organic Chemistry, Graduate School of Pharmaceutical Sciences, Tohoku University, Sendai, Miyagi 980-8577, Japan

Received March 10, 2022; Accepted April 6, 2022

DOI: 10.3892/etm.2022.11325

Abstract. Bioactive natural or phytoproducts have emerged as a potential source of antiviral agents. Of the *Rhus* spp., *R. coriaria* and *R. succedanea* have been reported for their antiviral activities against hepatitis B virus (HBV), while the anti-HBV efficacy of *R. tripartita* has remained elusive. In the present study, the anti-HBV activities of *R. tripartita*-derived novel catechin [3,5,13,14-flavan-3-yl-gallate or rhuspartin (RPT)] and epicatechin-3-*O*-rhamnoside (ECR), were assessed using the HBV-reporter cell line HepG2.2.15. RPT and ECR proved to efficiently inhibit HBV surface antigen (HBsAg) synthesis by 68.8 and 71.3%, respectively, and HBV pre-core antigen (HBeAg) production by 62.3 and 71.2%, respectively, after 5 days of treatment. Of note, RPT had a lower anti-HBV activity than ECR. In comparison, the reference drug lamivudine (LAM) inhibited HBsAg and HBeAg expression by 83.6 and 85.4%, respectively. Further molecular docking analysis revealed formations of strong complexes of RPT, ECR and LAM with HBV polymerase through interactions with binding pocket residues. Taken together, the present results demonstrated promising therapeutic potential of the novel *R. tripartita*-derived catechin and epicatechin for HBV, warranting their further molecular and pharmacological evaluation.

Introduction

The genus *Rhus* is widely distributed in tropical, subtropical and temperate regions, and several *Rhus* spp. are used for nutritional and medicinal purposes (1). Of these, *R. glabra* is used for bacterial infection (2), whereas *R. coriaria* is used for wound healing (3). In addition, *R. verniciflua* has been

demonstrated to possess strong antioxidant properties, attributed to its bioactive flavonoids, including quercetin, butein, fustin and sulfuretin (4,5). *R. tripartita* (Ucria) Grande, mainly distributed in North Africa and the Arabian Peninsula, is traditionally used for inflammatory, cardiovascular and gastrointestinal conditions (6-8). Further phytochemical and pharmacological studies of *Rhus* spp., including *R. tripartita*, have identified a variety of bioactive flavonoids, bioflavonoids and proanthocyanidins (1,9-11). Recently, a novel catechin along with epicatechin-3-*O*-rhamnoside from *R. tripartita* have been isolated (12).

Hepatitis B virus (HBV)-induced chronic liver diseases such as fulminant hepatitis, cirrhosis and carcinoma account for substantial morbidity and mortality (13). While several efficacious HBV-polymerase inhibitors (e.g., lamivudine, adefovir and acyclovir) are available, their long-term use frequently produces drug-resistant viral strains (14). To counter this issue, a range of natural bioactive flavonoids, polyphenols, alkaloids, terpenes, lignans and anthraquinones have been reported as potential anti-HBV agents with no sign of resistance (15-21). In line with these studies, *R. coriaria* has been demonstrated to have marked anti-HBV activity via inhibition of HBV surface or 's' antigen (HBsAg) secretion in cultured hepatoma cells (22). Recently, robustaflavone from *R. succedanea* has been reported as a potential inhibitor of HBV replication in HepG2.2.15 cells (23). However, to the best of our knowledge, the antiviral potential of *Rhus tripartita* or its bioactive constituents has so far remained elusive. Therefore, the present study assessed the anti-HBV efficacies of the *R. tripartita*-derived new catechin and epicatechin-3-*O*-rhamnoside, using *in vitro* as well as *in silico* approaches.

Materials and methods

Plant collection, extraction and isolation. *R. tripartita*, locally known as 'Sumac', was collected from Hail, Saudi Arabia and authenticated (voucher specimen no. SY 202/2013) by a plant taxonomist at College of Pharmacy, King Saud University (Riyadh, Saudi Arabia). The air-dried extract (80% ethanol) of the stem bark was further subjected to fractionation with ethyl acetate and sub-fractionated using column chromatography and thin-layer chromatography to yield

Correspondence to: Professor Mohammad K. Parvez, Department of Pharmacognosy, College of Pharmacy, King Saud University, 23 King Khalid Road, Riyadh 11451, Saudi Arabia
E-mail: mohkhalid@ksu.edu.sa

Key words: *Rhus tripartita*, hepatitis B virus, anti-HBV, catechin, epicatechin, HepG2.2.15 cell

two yellow-amorphous, powdery compounds as described previously (12). Subsequently, high-resolution electrospray ionization mass spectrometry (HRESIMS), ultraviolet (UV) and infrared (IR) spectroscopy, ^1H and ^{13}C DEPT-135 NMR spectroscopy, as well as 2D ^1H and ^{13}C heteronuclear single quantum correlation (HSQC) analyses were performed to determine their structures (12).

Cell culture and drugs. The human hepatoblastoma cell line HepG2 (ATCC HB-065) and its HBV-reporter derivative HepG2.2.15 (SCC249, Merck) were kind gift of Dr Shahid Jameel, Virology Group, International Center for Genetic Engineering & Biotechnology. Cells were cultured in RPMI-1640 medium (Gibco; Thermo Fisher Scientific Inc.) containing 10% fetal calf serum (Gibco; Thermo Fisher Scientific, Inc.) and 1X penicillin-streptomycin mix (HyClone; Cytiva) at 37°C with 5% CO_2 . HepG2.2.15 cells are HBV-infected HepG2 cells developed by stable transfection of HBV genomic DNA, which expresses all viral genes and proteins [e.g. HBsAg and HBV pre-core or 'e' antigen (HBeAg)], and are globally used to assess anti-HBV agents (24). The cells were further seeded (0.5×10^5 cells/100 μl /well) in a 96-well plate (Corning, Inc.) and incubated overnight prior to an assay. The approved HBV polymerase-inhibitor, lamivudine triphosphate (LAM; MilliporeSigma) and the anti-HBV flavonoid quercetin (QRC; MilliporeSigma) were used as a standard in cell culture studies as described elsewhere (20).

Cytotoxicity assay. The effect of *R. tripartita*-derived compounds (catechin and epicatechin) on HepG2 cells viability or toxicity was assessed using a TACS MTT Cell Proliferation Assay Kit (Bio-Techne) and the optimal safe doses were estimated. In brief, each compound was first dissolved in DMSO and then reconstituted in culture media to obtain four test concentrations or doses (10, 20, 30, 60 and 120 μM). HepG2 cells grown in a 96-well plate were replenished with fresh media containing the different drug doses or vehicle control (0.1% DMSO) and then incubated at 37°C for 72 h. All samples were tested in triplicate and the experiment was repeated twice. The optical density of the samples at 570 nm was recorded using a microplate reader (ELx800; BioTek Instruments, Inc.) and non-linear regression analysis was performed (Excel software 2010; Microsoft Corp.) to determine the 50% inhibitory concentration.

HBsAg inhibition assay. First, dose-dependent inhibition of HBsAg expression by the two test compounds (10, 20 and 30 μM each) was performed to determine the optimal active concentration. HepG2.2.15 cells grown in a 96-well plate were replenished with fresh media containing three selected doses of the compounds as well as controls, and incubated for 3 days. Following the determination of the optimal dose, a time-course inhibition of HBsAg expression by the two compounds was performed. Likewise, HepG2.2.15 cells were replenished with fresh media containing the optimal dose (30 μM each) of the compounds as well as controls, and incubated for up to 5 days. The culture supernatants were collected on days 1, 3 and 5 for analysis. The secretion of HBsAg into the culture supernatant was quantitatively analyzed using the diagnostic ELISA kit (cat. no. 72348;

MonolisaHBsAg ULTRA; Bio-Rad Laboratories Inc.) as per the manufacturer's protocol. The optical density of the samples at 450 nm was recorded using a microplate reader (ELx800; BioTek Instruments, Inc.), and analyzed in relation to the untreated control in Excel. All samples were tested in triplicate and the experiment was repeated twice.

HBeAg inhibition assay. The test compounds (30 μM) were evaluated for their time-course inhibitory effects on HBeAg synthesis. The post-treatment HepG2.2.15 supernatants collected on days 1, 3 and 5 were quantitatively analyzed for HBeAg expression using the diagnostic ELISA kit (cat. no. KAPG4BNE3; HBeAg/Anti-HBe Elisa Kit; DIAsource ImmunoAssays® S.A.) according to the manufacturer's protocol. The optical density of the samples at 450 nm was recorded using a microplate reader (ELx800; BioTek Instruments, Inc.), and analyzed in relation to the untreated control in Excel. All samples were tested in triplicate and the experiment was repeated twice.

Molecular docking analysis. For molecular docking analysis, an in-house constructed 3D structure of HBV polymerase (HBVpol) enzyme was used, as described in a previous study by our group (20). The 3D structures of LAM and co-crystallized entecavir triphosphate (ETV) were retrieved from the PubChem database (<https://pubchem.ncbi.nlm.nih.gov/>) and used as ligand controls. The 2D structures of the test compounds (ligands) were drawn in ChemDraw Pro 8.0 (chemistrydocs.com/chemdraw-pro-8-0/), following assignments of bond orders and bond angles. The structures of target protein (NCBI GenBank: AGA95798.1) was prepared and optimized using Maestro v12.3 LigPrep module (25), whereas the 2D and 3D visualizations of the ligand-target interactions were generated using University of California San Francisco ChimeraX (26). Prior to the docking of test compounds, any water molecules or bound hetero atoms were removed from the target. Further, the Gasteiger partial charges were defined and energies were minimized for all ligands in the Universal Force Field program (27). The docking analysis was performed on the target's binding sites in AutoDock Vina 1.2 operated in Linux OS (28). The docking protocol was validated by re-docking the co-crystallized ligands into the binding site and visual inspection and the Root Mean Square Deviation (RMSD) was calculated.

Statistical analysis. Data analysis was performed using the SPSS statistical package, version 17.0 (SPSS, Inc.). Data of all triplicate samples, expressed as the mean \pm standard error of the mean were analyzed by one-way ANOVA, followed by Dunnett's-test. $P < 0.05$ was considered to indicate a statistically significant difference.

Results and Discussion

Identification of isolated compounds. Of the several known anti-HBV natural flavonoids, including *R. succedanea*-derived robustaflavone, the flavonol catechin and derivatives have been also reported for antiviral activities against HBV (23,29). In line with this, the HRESIMS, UV/IR and ^1H - ^{13}C NMR spectroscopy, as well as 2D ^1H - ^{13}C HSQC analyses of

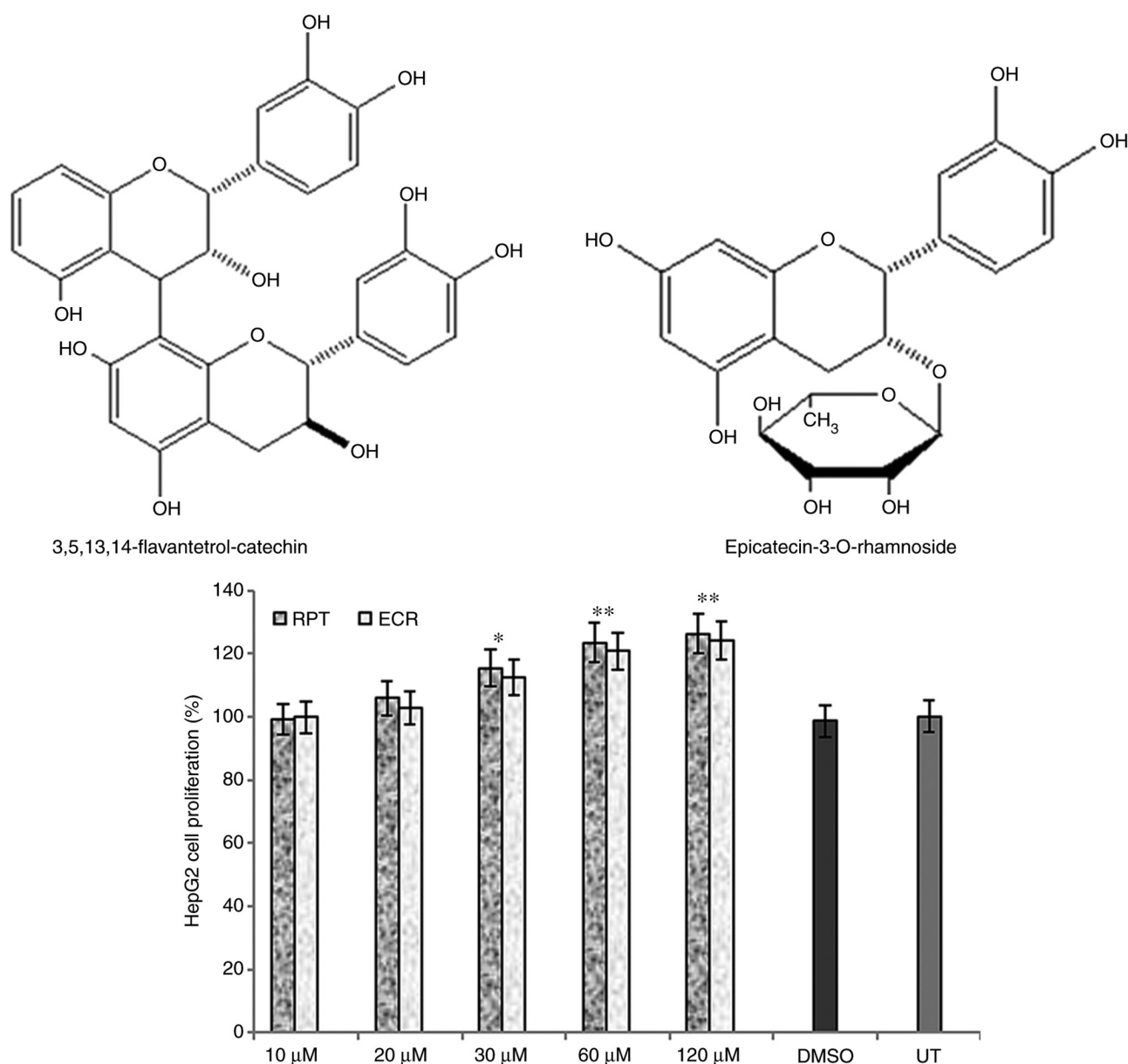


Figure 1. Chemical formulas of *R. tripartita*-derived catechins RPT and epicatechin ECR (upper panel) and their hepatocyte growth stimulatory activities on cultured HepG2 cells, where vehicle control (0.1% DMSO) and UT served as negative controls. Values are expressed as the mean \pm standard error of the mean (n=3). *P<0.05, **P<0.01 vs. UT (lower panel). UT, untreated control; ECR, epicatechin-3-O-rhamnoside; RPT, rhuspartin, 3,5,13,14-flavantetrol-catechin.

R. tripartita-derived compounds led to their identification as 3,5,13,14-flavantetrol-(4 β →8)-catechin (rhuspartin; RPT) and epicatechin-3-O-rhamnoside (ECR) (Fig. 1, upper panel), as described elsewhere (12).

Hepatocyte proliferative activities of the catechin and epicatechin. Prior to their anti-HBV assessments, RPT and ECR when tested on HepG2 cells and did not exhibit any cytotoxicity even at the maximal dose (120 μ M). Of note, while they had marginal growth stimulatory activities at 30 μ M, they exhibited significant but comparable growth enhancement at 60 and 120 μ M doses as compared to the untreated cells (P<0.01; Fig. 1, lower panel) on day 3. Therefore, further anti-HBV assays of RPT and ECR were conducted at 20 and 30 μ M doses, and not continued for longer than 5 days due to cell overgrowth and death.

Dose- and time-dependent inhibition of HBV antigen synthesis by RPT and ECR. RPT and ECR exhibited a dose-dependent anti-HBV activity, where the 20 and 30 μ M doses led to maximal activities as compared to the untreated cells (P<0.01; Fig. 2). As no significant differential activity was observed between the two doses, 30 μ M was selected as the optimal dose for the further analyses. In the time-dependent analysis of HBsAg, ECR and RPT suppressed its expression by 71.3% (P<0.01) and 68.8% (P<0.01), respectively whereas QRC inhibited it by 76.4% (P<0.001) as compared to the reference drug LAM on day 5 (Fig. 3). Furthermore, in the time-dependent analysis of HBeAg, ECR and RPT maximally downregulated its synthesis by 71.2% (P<0.01) and 62.3% (P<0.01), respectively, whereas QRC suppressed it by 75.4% (P<0.001) as compared to LAM on day 5 (Fig. 4). Thus, ECR had a marginally higher anti-HBV activity than

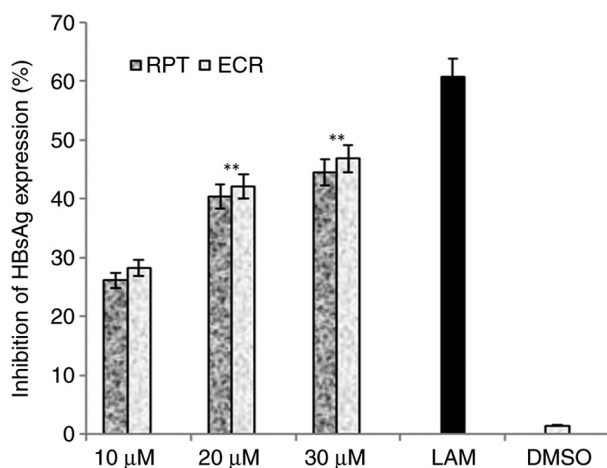


Figure 2. Anti-HBV assay indicating dose-dependent (10, 20 and 30 μ M) inhibition of HBsAg by *R. tripartita*-derived catechin RPT and epicatechin ECR in HepG2.2.15 cells. LAM (2 μ M) served as a positive control, while DMSO (0.1%) was used as a negative control. Values are expressed as the mean \pm standard error of the mean (n=3). **P<0.01 vs. LAM. HBsAg, HBV surface antigen; ECR, epicatechin-3-*O*-rhamnoside; RPT, rhuspartin, 3,5,13,14-flavanetrol-catechin; LAM, lamivudine triphosphate.

RPT. As RPT and ECR exerted growth stimulatory effects on HepG2 cells at 60 μ M or above on day 3 (Fig. 1, lower panel), a single optimal dose of 30 μ M was used in the antiviral assays performed for up to 5 days. As compared to LAM, incubating HepG2.2.15 cells with RPT and ECR at 30 μ M for longer than 5 days also enhanced cell growth (data not shown). In view of this, it was not possible to compare the anti-HBV effects of RPT and ECR with those of LAM due to differences in cell population and the amount of secreted HBV antigens, and incubation was therefore terminated a day 5. In previous studies, the antiviral activities of catechin derivatives such as epicatechin-3-gallate and epigallocatechin-3-gallate have been reported against herpes simplex virus, human immunodeficiency virus, human T-cell leukemia virus, Epstein-Barr virus, influenza virus, rotavirus and adenovirus as well as HBV and hepatitis C virus (16,29). In addition, a previous study by our group indicated moderate anti-HBV activities of *Oncocalyx glabratus*-derived catechin, catechin-7-*O*-gallate, catechin-7,4'-*O*-digallate and catechin-7,3'-*O*-digallate in HepG2.2.15 cells (30).

Structure-based virtual interaction of RPT and EPR with HBVpol. Molecular docking is a widely used *in silico* technique in drug discovery projects to predict the best conformation for a molecule and its potential affinity to a specific molecular target. As HBVpol enzyme is essential for HBV DNA replication, this enzyme remains an important drug target. Therefore, a molecular docking technique was employed to support the *in vitro* data towards delineating the possible mechanisms of anti-HBV activity of the isolated catechin and epicatechin. The good re-alignment of the co-crystallized ligand ETV prior to and after docking inside the binding cavity of HBVpol along with the low RMSD values between the two structures indicated a valid docking protocol (Fig. 5, upper panel). Furthermore, the docked complex of LAM-HBVpol was observed to adopt a conformation quite similar to that of the ETV-HBVpol complex (Fig. 5, lower panel), confirming

Table I. Estimated docking energies of *R. tripartita*-derived compounds and standard drugs against HBV polymerase.

Compound	Docking energy, kcal/mol
Rhuspartin ^a	-7.949
Epicatechin-3- <i>O</i> -rhamnoside ^a	-8.483
Lamivudine triphosphate ^b	-9.245
Entecavir triphosphate ^b	-8.212

^a*R. tripartita*-derived compound; ^bstandard.

robustness and reliability of the protocol. The estimated binding free energies for the ETV-HBVpol and LAM-HBVpol complex were -8.21 and -9.24 kcal/mol, respectively (Table I). Furthermore, RPT and ECR exhibited affinity for the HBVpol in proximity of its 'Tyr-Met-Asp-Asp (YMDD)' motif, similar to LAM (Fig. 6). In addition to the 'YMDD' motif, Lys14, Ser67 and Ala68 also surrounded the ligand compounds, which may potentially contribute to ligand-target complex stabilities. In addition, both compounds adopted relatively similar orientations and aligned inside the active site of HBVpol as compared to the control ligands. ECR engaged in interactions with the key residues of HBVpol, including a hydrogen bonding with a charged Arg23 residue, a face-to-face π -stacking with the nucleotides of the DNA and a metal coordination with an Mg²⁺ ion embedded inside the pocket (Fig. 6). It is thought that coordination with Mg²⁺ ions has an integral part in stabilizing a ligand-target complex (31). By contrast, the only key interaction of RPT was its metal coordination by Mg²⁺. However, ECR exhibited a better binding affinity as compared to RPT, which may be attributed to the hydrophobic contact between the ligand and the target (Fig. 5). Though slightly lower than that for LAM, the calculated binding free energies for ECR and RPT were -8.483 and -7.949 kcal/mol, respectively (Table I).

Flavonoids are plant phenols, which, according to their variations in their heterocyclic carbon (C₆-C₃-C₆) ring, have been classified as flavones, flavonols, flavanones, isoflavones, anthocyanidins and catechins (32). Of note, the compounds examined in the present study belong to the subclass of 'catechins', where ECR is a monomeric (epi)catechin conjugated with a sugar moiety i.e., glycone, and RPT is a dimeric catechin, i.e., aglycon (Fig. 1, upper panel). In view of the structure-activity relationship of the compounds, the observed marginal difference in the bioactivity of ECR and RPT may therefore be attributed to the differences in their chemical structures. Furthermore, in the metabolic process, a glycone is generally poorly absorbed as compared to its aglycone counterpart (32). However, hydrolysis of the glycone furnishes a free aglycone, which easily gets absorbed and performs its activity. By contrast, the breakdown of a dimeric aglycone is relatively difficult and therefore, it has poor absorption and low activity. Taken together, this information strongly supports the differential structure-activity of the studied catechin and epicatechin.

In conclusion, the present data, for the first time, demonstrated the promising anti-HBV therapeutic potential of the *R. tripartita*-derived compounds ECR and RPT in an

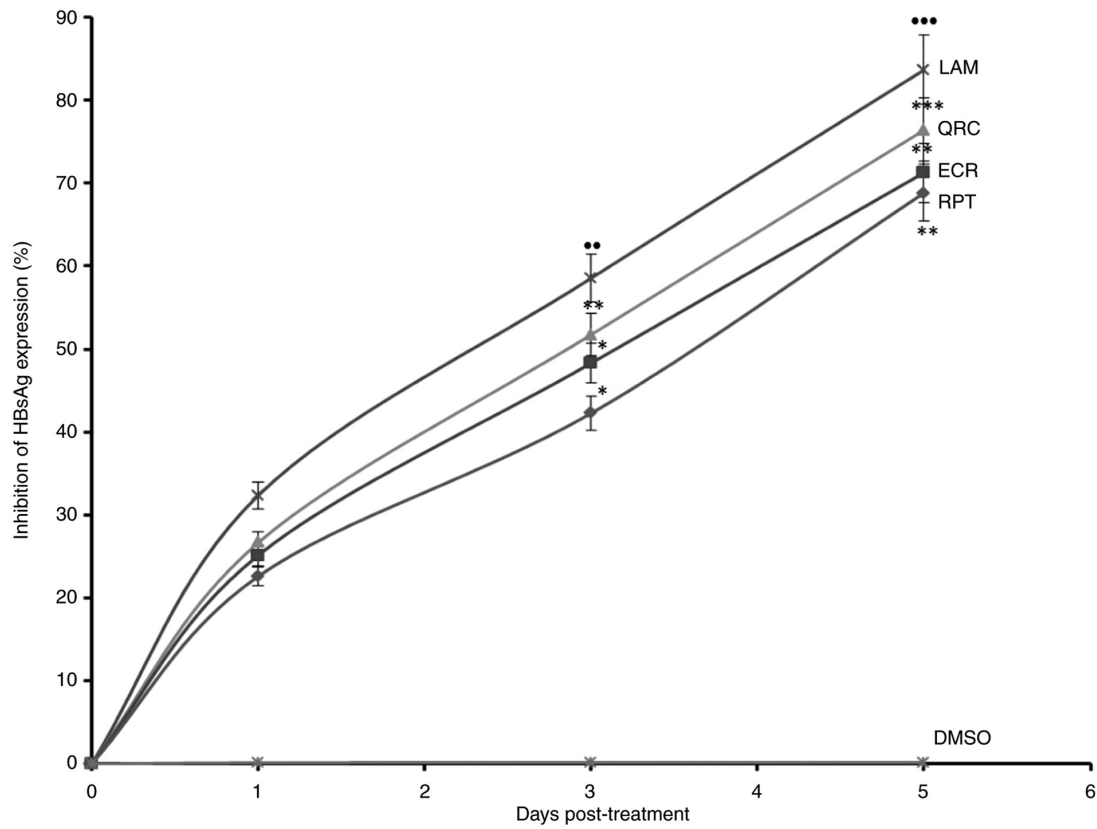


Figure 3. Anti-HBV assay indicating time-dependent inhibition of HBsAg by *R. tripartita*-derived catechin RPT (30 μM) and epicatechin ECR (30 μM) in HepG2.2.15 cells. LAM (2 μM) and QRC (27 μM) served as positive controls, while DMSO (0.1%) was used as an NC. Values are expressed as the mean ± standard error of the mean (n=3). **P<0.01, ***P<0.001 vs. NC; *P<0.05, **P<0.01, ***P<0.001 vs. LAM. QRC, quercetin; NC, negative control; HBsAg, HBV surface antigen; ECR, epicatechin-3-*O*-rhamnoside; RPT, rhuspartin, 3,5,13,14-flavanterol-catechin; LAM, lamivudine triphosphate.

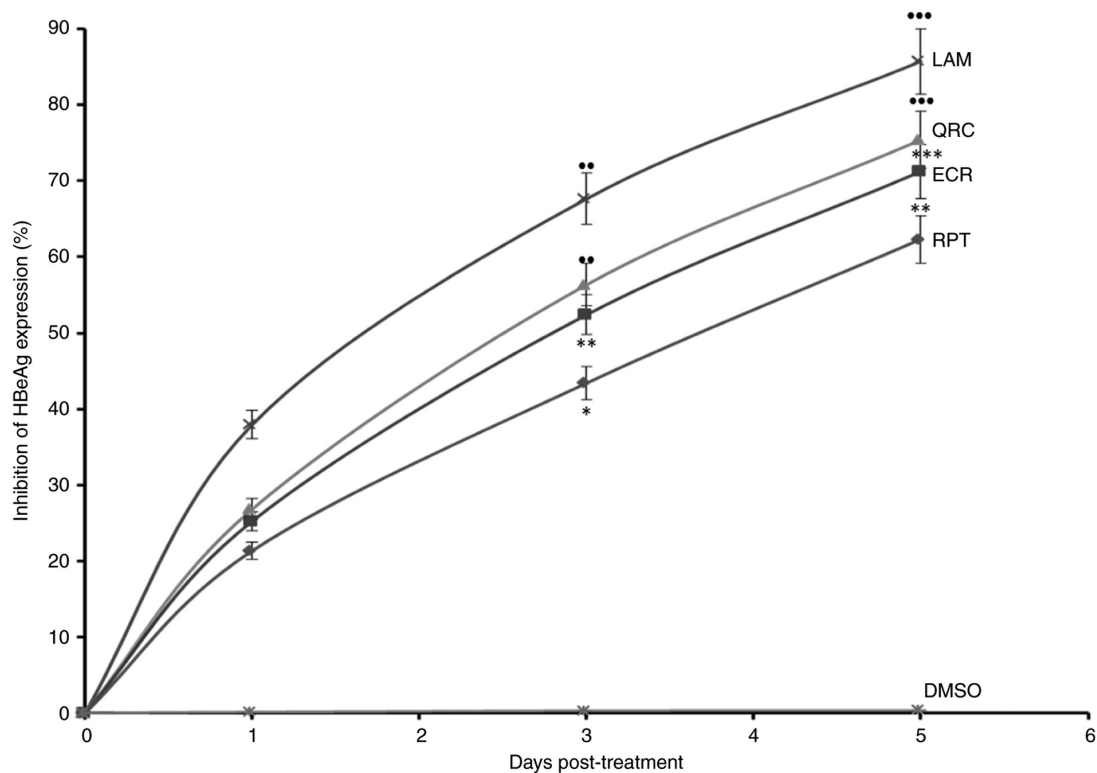


Figure 4. Anti-HBV assay demonstrating time-dependent inhibition of HBeAg by *R. tripartita*-derived catechin RPT (30 μM) and epicatechin ECR (30 μM) in HepG2.2.15 cells. LAM (2 μM) and QRC (27 μM) served as positive controls, while DMSO (0.1%) acted as NC. Values are expressed as the mean ± standard error of the mean (n=3). **P<0.01, ***P<0.001 vs. BC. *P<0.05, **P<0.01, ***P<0.001 vs. LAM. HBeAg, HBV pre-core or 'e' antigen; QRC, quercetin; NC, negative control; ECR, epicatechin-3-*O*-rhamnoside; RPT, rhuspartin, 3,5,13,14-flavanterol-catechin; LAM, lamivudine triphosphate.

HBV-reporter cell culture model, supported by molecular docking analysis. This warrants their further molecular and pharmacological study towards developing novel and efficacious natural therapeutics against HBV infection.

Acknowledgements

Not applicable.

Funding

The authors gratefully acknowledge the Researchers Supporting Project (grant no. RSP-2021/379), King Saud University (Riyadh, Saudi Arabia) for supporting this work.

Availability of data and materials

The datasets used and/or analyzed during the current study are available from the corresponding author on reasonable request.

Authors' contributions

MKP and MSAD conceptualized and designed the study, performed *in vitro* assays, collected and analyzed data and wrote the manuscript. MASA performed the *in silico* analysis and contributed to manuscript writing. ASA and ARA prepared the compounds and performed statistical analysis. MKP and MASA confirm the authenticity of all the raw data. All authors have read and approved the final manuscript.

Ethics approval and consent to participate

Not applicable.

Patient consent for publication

Not applicable.

Competing interests

The authors declare that they have no competing interests.

References

- Opiyo SA, Njoroge PW, Ndirangu EG and Kuria KM: A review of biological activities and phytochemistry of *Rhus* Species. *Am J Chem* 11: 28-36, 2021.
- Erichsen-Brown C: Medicinal and Other uses of North American Plants: A Historical Survey with Special Reference to the Eastern Indian Tribes. Dover Publications, Mineola, NY, 1989.
- Sezik E, Tabata M, Yesilada E, Honda G, Goto K and Ikeshiro Y: Traditional medicine in Turkey. Folk medicine in Northeast Anatolia. *J Ethnopharmacol* 35: 191-196, 1991.
- Jang JY, Shin H, Lim JW, Ahn JH, Jo YH, Lee KY, Hwang BY, Jung SJ, Kang SY and Lee MK: Comparison of antibacterial activity and phenolic constituents of bark, lignum, leaves and fruit of *Rhus verniciflua*. *PLoS One* 13: e0200257, 2018.
- Kang SY, Kang JY and Oh MJ: Antiviral activities of flavonoids isolated from the bark of *Rhus verniciflua* stokes against fish pathogenic viruses in vitro. *J Microbiol* 50: 293-300, 2012.
- Itidel C, Chokri M, Mohamed B and Yosr Z: Antioxidant activity, total phenolic and flavonoid content variation among Tunisian natural populations of *Rhus tripartita* (Ucria) Grande and *Rhus pentaphylla* Desf. *Ind Crops Prod* 51: 171-177, 2013.
- El-Mokasabi F: The state of the art of traditional herbal medicine in the Eastern mediterranean coastal region of Libya. *Middle East J Sci Res* 21: 575-582, 2014.
- Shahat AA, Alsaïd MS, Rafatullah S, Al-Sohaibani MO, Parvez MK, Al-Dosari MS, Exarchou V and Pieters L: Treatment with *Rhus tripartita* extract curtails isoproterenol-elicited cardiotoxicity and oxidative stress in rats. *BMC Complement Altern Med* 16: 351, 2016.
- Mahjoub MA, Ammar S and Mighri Z: A new biflavonoid and an isobiflavonoid from *Rhus tripartitum*. *Nat Prod Res* 19: 723-729, 2005.
- Alimi H, Mbarki S, Barka ZB, Feriani A, Bouoni Z, Hfaïdh N, Sakly M, Tebourbi O and Rhouma KB: Phytochemical, antioxidant and protective effect of *Rhus tripartitum* root bark extract against ethanol-induced ulcer in rats. *Gen Physiol Biophys* 32: 115-127, 2013.
- Mohammed AE-SI: Phytoconstituents and the study of antioxidant, antimalarial and antimicrobial activities of *Rhus tripartita* growing in Egypt. *J Pharmacogn Phytochem* 4: 276-281, 2015.
- Alqahtani AS, Abdel-Mageed WM, Shahat AA, Parvez MK, Al-Dosari MS, Malik A, Abdel-Kader MS and Alsaïd MS: Proanthocyanidins from the stem bark of *Rhus tripartita* ameliorate methylglyoxal-induced endothelial cell apoptosis. *J Food Drug Anal* 27: 758-765, 2019.
- Tang LSY, Covert E, Wilson E and Kottlil S: Chronic hepatitis B infection: A review. *JAMA* 319: 1802-1813, 2018.
- Devi U and Locarnini S: Hepatitis B antivirals and resistance. *Curr Opin Virol* 3: 495-500, 2013.
- Wang G, Zhang L and Bonkovsky HL: Chinese medicine for treatment of chronic hepatitis B. *Chin J Integr Med* 18: 253-255, 2012.
- Parvez MK, Arab AH, Al-Dosari MS and Al-Rehaily AJ: Antiviral natural products against chronic hepatitis B: Recent developments. *Curr Pharm Des* 3: 286-293, 2016.
- Parvez MK, Tabish Rehman M, Alam P, Al-Dosari MS, Alqasoumi SI and Alajmi MF: Plant-derived antiviral drugs as novel hepatitis B virus inhibitors: Cell culture and molecular docking study. *Saudi Pharm J* 27: 389-400, 2019.
- Parvez MK, Al-Dosari MS, Alam P, Rehman M, Alajmi MF and Alqahtani AS: The anti-hepatitis B virus therapeutic potential of anthraquinones derived from Aloe vera. *Phytother Res* 33: 2960-2970, 2019.
- Parvez MK, Al-Dosari MS, Arbab AH, Al-Rehaily AJ and Abdelwahid MAS: Bioassay-guided isolation of anti-hepatitis B virus flavonoid myricetin-3-O-rhamnoside along with quercetin from *Guiera senegalensis* leaves. *Saudi Pharm J* 28: 550-559, 2020.
- Parvez MK, Ahmed S, Al-Dosari MS, Abdelwahid MAS, Arbab AH, Al-Rehaily AJ and Al-Oqail MM: Novel Anti-Hepatitis B virus activity of *Euphorbia schimperii* and its quercetin and kaempferol derivatives. *ACS Omega* 6: 29100-29110, 2021.
- Parvez MK, Al-Dosari MS, Rehman MT, Al-Rehaily AJ, Alqahtani AS and Alajmi MF: The anti-hepatitis B virus and anti-hepatotoxic efficacies of solanopubamine, a rare alkaloid from *Solanum schimperianum*. *Saudi Pharm J*: Feb 7, 2022 (Epub ahead of print). doi: <https://doi.org/10.1016/j.jsps.2022.02.001>.
- Amin FG, Farzaneh S, Mohsen K, Mohammad K, Hessam M, Dawood MNS and Ali AN: Effects of *Rhus Cortaria* L. (Sumac) extract on hepatitis B virus replication and HBs Ag secretion. *J Rep Pharm Sci* 7: 100-107, 2018.
- Zembower DE, Lin YM, Flavin MT, Chen FC and Korba BE: Robustflavone, a potential non-nucleoside anti-hepatitis B agent. *Antiviral Res* 39: 81-88, 1998.
- Sells MA, Chen ML and Acs G: Production of hepatitis B virus particles in Hep G2 cells transfected with cloned hepatitis B virus DNA. *Proc Natl Acad Sci USA* 84: 1005-1009, 1987.
- Schrödinger Release 2022-1: Maestro, Schrödinger, LLC, New York, NY, 2021.
- Goddard TD, Huang CC, Meng EC, Pettersen EF, Couch GS, Morris JH and Ferrin TE: UCSF ChimeraX: Meeting modern challenges in visualization and analysis. *Protein Sci* 27: 14-25, 2018.
- Eberhardt J, Santos-Martins ED, Tillack AF and Forli F: AutoDock Vina 1.2.0: New docking methods, expanded force field, and python bindings. *J Chem Inf Model* 61: 3891-3898, 2021.
- Trott O and Olson AJ: AutoDock Vina: Improving the speed and accuracy of docking with a new scoring function, efficient optimization, and multithreading. *J Comput Chem* 31: 455-461, 2010.

29. Badshah SL, Faisal S, Muhammad A, Poulson BG, Emwas AH and Jaremko M: Antiviral activities of flavonoids. *Biomed Pharmacother* 40: 111596, 2021.
30. Ahmed S, Al-Rehaily AJ, Ahmad MS, Yousaf M, Alam MN, Parvez MK, Al-Dosari MS, Noman OM, Khan SI and Khan IA: Chemical constituents from *Oncocalyx glabratus* and their bioactivities. *Phytochemistry Lett* 20: 128-132, 2017.
31. Bertolotti N, Chan AH, Schinazi RF, Yin YW and Anderson KS: Structural insights into the recognition of nucleoside reverse transcriptase inhibitors by HIV-1 reverse transcriptase: First crystal structures with reverse transcriptase and the active triphosphate forms of lamivudine and entecavir. *Protein Sci* 28: 1664-1675, 2019.
32. Hollman PCH: Absorption, bioavailability and metabolism of flavonoids. *Pharm Biol* 42: 74-83, 2004.